

as a function of energy was compared with the results of others. The small trend toward lower populations of defects in I_B and I_C with increasing electron energy is supported. It may be necessary to review the significance of the change at lower energy^{3,5} since the present experiment has shown that I_B actually consists of two substages, I_2 and I_3 .

Further work is required to relate the eight or nine substages to the corresponding detailed recombination process together with the determination of the stable interstitial configuration in copper. Such work is now in progress.

A comparison of the new recovery spectrum of copper with that of gold indicates that the first few substages of recovery are due to the same processes,

hence, many of the same types of defects are produced, only in different concentrations in the two metals.

ACKNOWLEDGMENTS

The authors wish to thank Dr. R. M. Walker for use of his specimens and cryostat (which was modified) and for the generous amount of his time spent in discussions and in suggestions. Mrs. E. L. Fontanella of GE Labs is thanked for her suggestions on some experimental techniques. The conscientious help of R. C. Erwood, L. A. Watson, J. Scott-Monck, and K. O. Koestler is gratefully acknowledged.

Dr. E. N. Strait and H. H. Hagelauer are thanked for their cooperation concerning the operations at the Northwestern Nuclear Physics Research Laboratory.

Experiments on Stage III Annealing in the Noble Metals*

F. DWORSCHAK, K. HERSCHBACH,† AND J. S. KOEHLER

Department of Physics, University of Illinois, Urbana, Illinois

(Received 26 August 1963)

High purity copper, silver, and gold specimens have been irradiated with 10-MeV protons near 80°K. An integrated flux of 1×10^{17} p/cm^2 produced a resistivity increase of 3.3×10^{-8} $\Omega\text{-cm}$ in copper, 7.4×10^{-8} $\Omega\text{-cm}$ in silver, and 16.6×10^{-8} $\Omega\text{-cm}$ in gold. The specimens were isothermally annealed in steps of 20°K for 64 min at each temperature from 143 to 363°K. The recovery in stage III follows second-order kinetics with an activation energy of 0.71 ± 0.04 eV for copper, 0.67 ± 0.03 eV for silver, and 0.80 ± 0.04 eV for gold. Distribution curves of the fractional concentration of defects annealing with a given activation energy have been calculated. In the case of copper and silver they show a complex structure followed by a large broad maximum at 0.71 eV for copper and 0.67 eV for silver. In gold there is only one large peak at 0.80 eV. The relationship of these results to the various models is discussed.

I. INTRODUCTION

THE recovery of the electrical resistivity change which occurs in irradiated noble metals in the range from 200 to 300°K (stage III) has been studied in a number of experiments, but only few kinetic measurements have been made. Overhauser¹ measured the isothermal annealing of 99.99% pure copper irradiated with 12-MeV deuterons at 100°K. He observed a recovery process that had an activation energy of 0.68 eV and that obeyed a chemical rate equation of 2.5 order. Meechan and Brinkman² and Meechan, Sosin, and Brinkman³ irradiated high purity copper with 1.25-MeV electrons at 80°K and investigated the recovery of the electrical resistivity change upon annealing. They found a second-order process

with an activation energy of 0.60 eV. Kauffman⁴ reports a recovery process with an activation energy of 0.72 ± 0.05 eV in gold after electron irradiation near 100°K.

Various models have been proposed to explain the recovery in stage III, but it is still uncertain what the nature of this recovery process is. Following are the possibilities which have been suggested: migration of a vacancy; migration of a divacancy; migration of a second kind of interstitial; migration of a diinterstitial; and breakup of interstitial complexes.

In the case of gold the energy of motion of a single vacancy is known to be⁵ 0.82 ± 0.05 eV and that of a divacancy 0.64 ± 0.04 eV,⁶ and in the case of silver the energy of motion of a single vacancy 0.83 ± 0.05 eV,⁷ and that of a divacancy 0.57 ± 0.03 eV.⁷

The present research was carried out with the hope that it might clarify this situation by comparing the

* Research supported by the United States Atomic Energy Commission.

† Present address: Missile and Space Systems Division, Douglas Aircraft Company, Inc., Santa Monica, California.

¹ A. W. Overhauser, *Phys. Rev.* **90**, 393 (1953).

² C. J. Meechan and J. A. Brinkman, *Phys. Rev.* **103**, 1193 (1956).

³ C. J. Meechan, A. Sosin, and J. A. Brinkman, *Phys. Rev.* **120**, 411 (1960).

⁴ J. W. Kauffman, AEC Report TID-14745 (unpublished).

⁵ J. E. Bauerle and J. S. Koehler, *Phys. Rev.* **107**, 1493 (1957).

⁶ W. Palmer and J. S. Koehler, *Bull. Am. Phys. Soc.* **3**, 366 (1958).

⁷ M. Doyama and J. S. Koehler, *Phys. Rev.* **127**, 21 (1962).

activation energy spectra in stage III of irradiated copper, silver, and gold. The specimens were bombarded near 80°K with 10-MeV protons in the Illinois cyclotron and subsequently subjected to a series of isothermal anneals. The changes in electrical resistivity with time were measured during each step of thermal treatment.

II. METHOD AND APPARATUS

Experimentally one wishes to bombard a number of metal specimens near liquid-nitrogen temperature, obtaining damage concentrations which are much larger than the impurity concentration, then to anneal the specimens at constant temperature. The progress of the annealing is followed by measuring the change in the electrical resistivity of the specimens at 4.2°K. To achieve this the specimens were mounted on a cylindrical aluminum block. The specimens span a square hole which extends through the aluminum block. The external faces of the block were covered by one-mil aluminum foil windows. The assembly could be filled with gaseous helium through an aluminum tube. Potential and current leads were brought out through a second tube. Each assembly contained two specimens and the entire assembly was moved from a liquid nitrogen-irradiation jig to a constant temperature bath, and from there to a liquid helium double Dewar. In this way no warmup occurred during transfer from irradiation jig to annealing bath or in the other necessary transfers. In addition, the specimens were not subject to cold work. The construction of the specimens holder assembly and of the irradiation jig will be described in detail elsewhere.⁸

The constant temperature bath was kept in a cryostat similar to that described by Scott and Brickwedde.⁹ Below 280°K the bath was a nonflammable liquid¹⁰ with a freezing point of 128°K and above 280°K water was used. The liquid was cooled by liquid nitrogen at low temperatures. Above 20°C icewater was used. Temperature equilibrium was achieved by means of a regulated electric heater. The temperature of the bath was monitored with a platinum resistance thermometer and could be held constant to within $\pm 0.02^\circ\text{C}$ during any anneal.

Standard potentiometric methods were used to determine the resistance of the specimens. A 1000-0.1 Ω -decade resistor and a home-made 0.01 Ω -decade resistance unit were used to adjust the current through the specimen. The current was monitored with a Leeds and Northrup type K-3 potentiometer by measuring the voltage drop across a 1- Ω standard resistor connected in series with the specimen. The value of the current

was 0.2 A. It was regulated to better than 1 part in 10 000. The voltage drop across the specimen was measured using a Rubicon 6-dial-microvolt potentiometer with a photoelectric galvanometer acting as a null detector. The parasitic emf's in the circuit were eliminated by reversing the current through the specimen and taking an average reading. The experimental error in the resistivity measurements was smaller than $1 \times 10^{-12} \Omega\text{-cm}$.

III. SPECIMEN MOUNTING AND PREPARATION

The specimens used in this experiment were 5-mil-diam wires approximately 10 cm long. They were bent zig-zag and the cusps of the specimens were spotwelded to a frame cut from a 2.5-mil foil of the same material [Figs. 1(a) and 1(b)]. Short 5-mil current and potential leads were spotwelded to the ends of the specimens. Frames, current and potential leads were always made from the same material as the specimen. This kind of mounting reduced the cold work after the anneal and during the mounting to a minimum. The entire frame was annealed and mounted in the method described by Herschbach.¹¹ After the frames were securely mounted on the specimen holder, the four sides of the frame were cut off and removed without disturbing the specimen having only the tabs as shown in Fig. 1(c).

The gold specimens were 5-mil-diam 99.999% pure Au wire supplied by Sigmund Cohn. Before and after mounting on the frame they were cleaned with acetone, methanol, boiling distilled water, HNO_3 and HCl . They were annealed for two hours at 700°C in air. The residual resistivity of the mounted gold specimens was less than $1.7 \times 10^{-9} \Omega\text{-cm}$.

The copper specimens were prepared from 99.999% pure Cu obtained from the American Smelting and Refining Company in the form of a $\frac{3}{8}$ -in. rod. This rod was swaged down to 50 mil and then drawn to 5-mil-diam wire. The material was etched with HNO_3 , and cleaned with KCN after every other swaging and drawing operation. The mounted specimens were etched and then annealed on spectroscopically pure graphite boats in vacuum (better than 1×10^{-6} mm Hg) at 530°C for two hours. The residual resistivity of the mounted copper specimens was lower than $1.67 \times 10^{-9} \Omega\text{-cm}$.

The material for the silver specimens was Tadanac

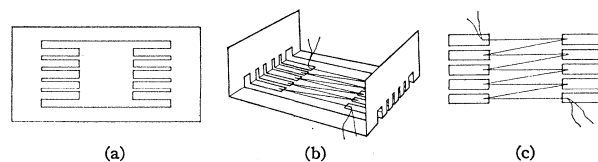


FIG. 1. (a) Shape of mounting frame; (b) spotwelded specimen; (c) specimen mounted on block.

⁸ F. Dworschak, K. Herschbach, and F. L. E. Witt, *Rev. Sci. Instr.* (to be published).

⁹ R. B. Scott and F. G. Brickwedde, *Bur. Std. J. Res.* **6**, 401 (1931).

¹⁰ C. W. Kanolt, *Sci. Papers Natl. Bur. Std. (U.S.)* **20**, 619 (1926).

¹¹ K. Herschbach, *Phys. Rev.* **130**, 554 (1963).

Brand 99.9999% pure Ag¹² supplied in the form of a $\frac{1}{8}$ -in. rod from Cominco Products, Inc. This rod was swaged and drawn to 5-mil-diam wire. The silver wire was etched with HNO₃ after every second swaging and drawing operation. After mounting, the specimens were etched again and then annealed in vacuum (better than 1×10^{-6} mm Hg) at 650°C for 2 h. The residual resistivity of the mounted silver specimens was less than 1.8×10^{-9} Ω-cm.

IV. PROCEDURE

The cryostat was visually aligned with respect to the proton beam and an electrically insulated Faraday cup was mounted to measure the proton beam. The beam uniformity was checked using a probe¹³ which could be driven across the cyclotron beam before it entered the cryostat. The intensity over the target area was constant to within 10%.

To measure the temperature rise during irradiation a dummy specimen with a thermocouple attached to the irradiated portion was also mounted on the block. The thermal emf was amplified using a Leeds and Northrup dc amplifier and recorded. The proton beam was adjusted so that the temperature of the dummy specimen was always lower than 110°K.

The dummy specimen was also used to check how rapidly the dummy reached the bath temperature when the block was immersed in the annealing bath. Since it took the specimens one minute at the most to acquire the temperature of the bath to within 0.02°C, the total annealing time was accordingly corrected by determining an approximate activation energy with the slope method and using this value to calculate an equivalent heating time.

V. DATA

Six irradiation runs, one for each sample holder, were performed using 10-MeV protons. In three of the runs the samples were exposed to an integrated flux of 1×10^{17} p/cm² producing a resistivity increase of 3.3×10^{-8} Ω-cm in Cu, 7.4×10^{-8} Ω-cm in Ag, and 1.66×10^{-7} Ω-cm in Au.

In the other three runs the integrated flux was 3.3×10^{16} p/cm² causing a resistivity increase of 1.8×10^{-8} Ω-cm in Cu, 4.25×10^{-8} Ω-cm in Ag, and 6.8×10^{-8} Ω-cm in Au.

The specimens that were exposed to the total flux of 1×10^{17} p/cm² and the copper specimens with a dose of 3.3×10^{16} p/cm² were subsequently isothermally annealed for 64-min periods at temperatures successively 20°K apart from 143 to 363°K. Above 300°K the annealing time was less than 64 min. The resistivity decrease with time during each anneal at one tempera-

ture was measured by taking the specimens out of the constant temperature bath and measuring the resistivity in liquid helium. These measurements were performed after 2, 4, 8, 16, 32, and 64 min total annealing.

The isochronal annealing curves for Cu, Ag, and Au irradiated with 1×10^{17} p/cm² (Fig. 2) show a gradual recovery rate, followed by a rapid annealing process in the temperature range from 200 to 300°K. Above 300°K recovery again proceeds at extremely slow rates. These observations are in agreement with the measurements of Cooper, Koehler, and Marx.¹⁴

To illustrate this behavior in detail the slope of the isochronal annealing curve has been plotted as a function of temperature. Large peaks, which indicate maximum annealing rates, occur at 243°K in copper [Fig. 3(a)], 233°K in silver [Fig. 3(b)], and 263°K in gold [Fig. 3(c)]. There is a small maximum at 183°K in gold. The portion of the resistance increase which recovers in the main peak was 59% for copper, 56% for silver, and 71% for gold. Up to 343°K 76% of the damage anneals out in copper, 78% in silver and 86% in gold.

The isothermal annealing curves for copper are given in Fig. 4(a), for silver in Fig. 4(b), and for gold in Fig. 4(c). Activation energies associated with these recovery processes were determined by observing the change in the annealing rate after a sudden increase of the annealing temperature T_i to T_{i+1} (slope method). This method has been used by Overhauser¹ for the calculation of activation energies and has been discussed by Dienes and Vineyard.¹⁵ The results seem to indicate that the annealing in stage III is caused by a single unique recovery process, having an activation

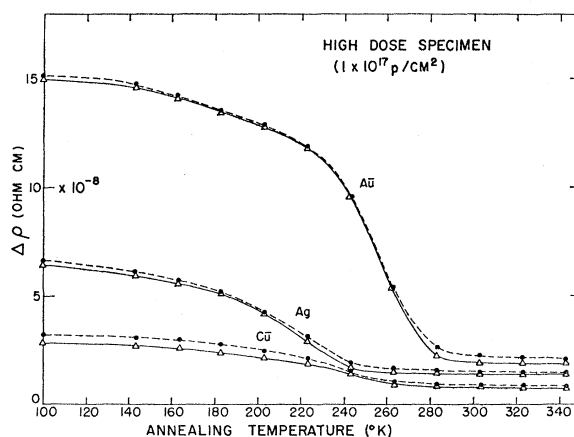


FIG. 2. Isochronal recovery of the electrical resistivity increase ($\Delta\rho$) for Cu, Ag, and Au specimens irradiated with 1×10^{17} p/cm². Two samples of each material were simultaneously irradiated and annealed.

¹⁴ H. G. Cooper, J. S. Koehler, and J. W. Marx, *Phys. Rev.* **97**, 599 (1955).

¹⁵ G. J. Dienes and G. H. Vineyard, *Radiation Effects in Solids* (Interscience Publishers, Inc., New York, 1957).

¹² Spectrographic analysis of the silver supplied by Cominco Products, Inc. Parts per million: 0.1 Ca, 0.1 Mg, 0.3 Si, 0.1 Al, 0.2 B, 0.1 Fe.

¹³ T. G. Nilan, doctoral thesis, Urbana, Illinois, 1961 (unpublished).

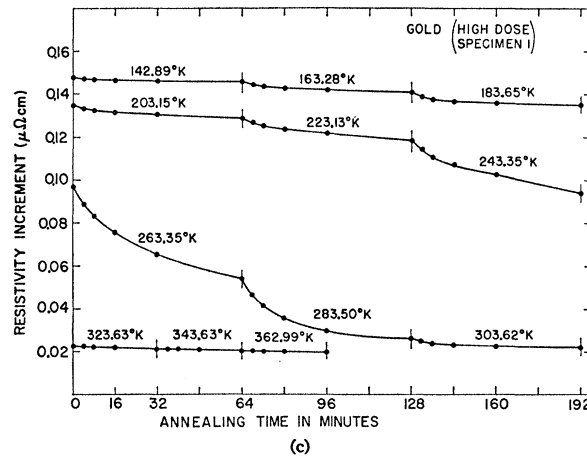
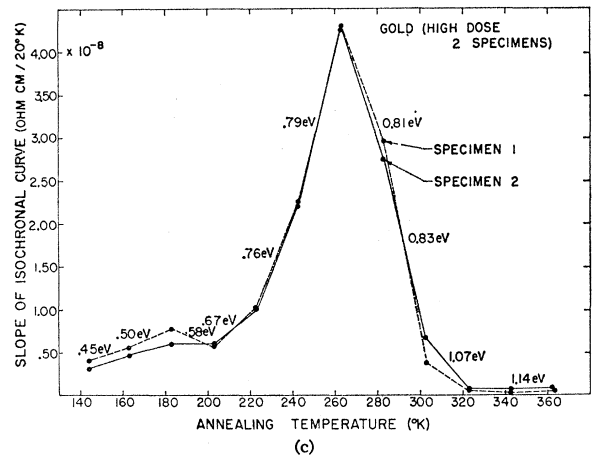
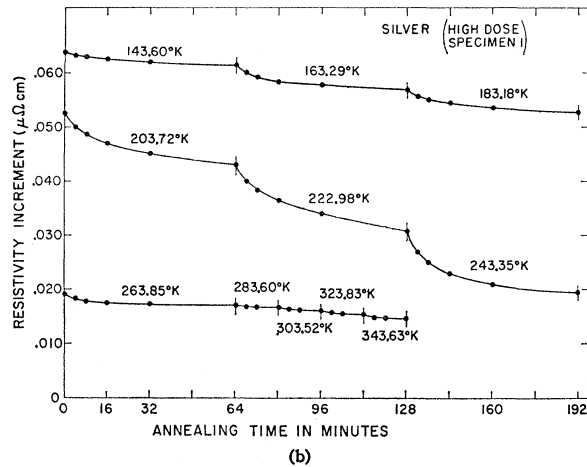
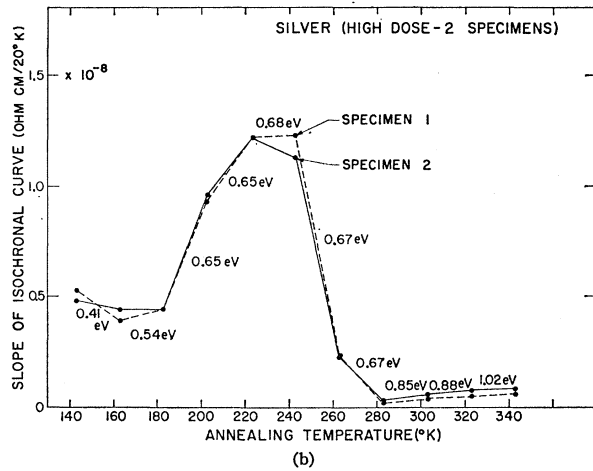
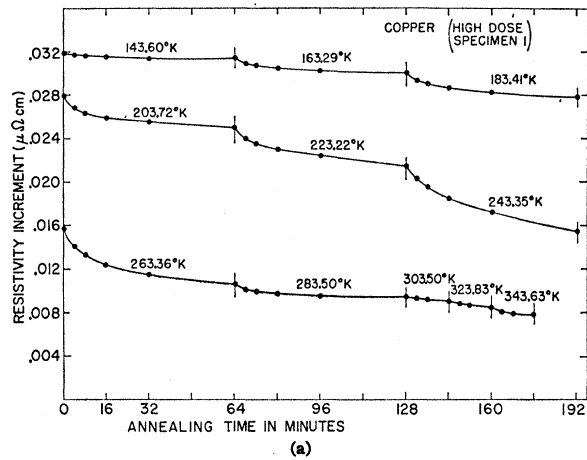
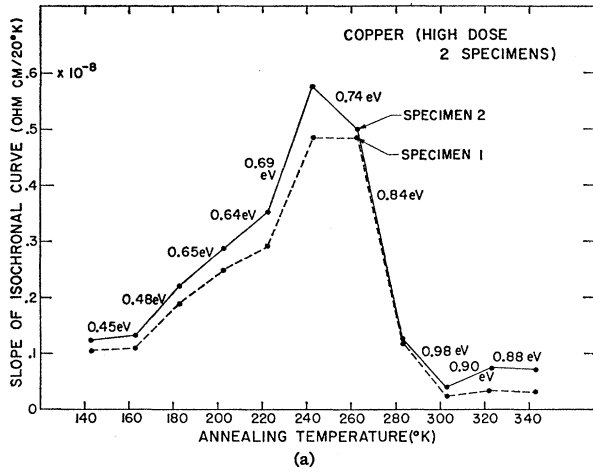


FIG. 3. Slope of isochronal recovery curves for (a) Cu; (b) Ag; and (c) Au irradiated with 1×10^{17} p/cm². Parameters are activation energies as determined by the slope method.

energy of 0.71 ± 0.04 eV in copper, 0.67 ± 0.03 eV in silver, and 0.80 ± 0.04 eV in gold. The values of the calculated activation energies as a function of temperature are shown as parameters on the isochronal

FIG. 4. Isothermal annealing data for (a) Cu; (b) Ag; and (c) Au irradiated with 1×10^{17} p/cm². Parameters are annealing temperatures.

curves [Figs. 3(a), 3(b), 3(c)]. Each number is an average of the calculated activation energies of two specimens.

An attempt was made to determine the order of reaction for these unique recovery processes. In previ-

ous experiments second-order and 2.5-order processes have been found. Therefore an investigation was made to determine whether this annealing behavior can be described by a second-order process.

Second-order reaction kinetics can be represented by the differential equation

$$d\Delta\rho/dt = -B(\Delta\rho)^2, \quad (1)$$

where $\Delta\rho = \rho - \rho_\infty$ and ρ_∞ is the asymptote of the isothermal annealing curve. The solution of this differential equation is

$$(\rho - \rho_\infty)^{-1} - (\rho_0 - \rho_\infty)^{-1} = Bt, \quad (2)$$

where ρ_0 is the value of ρ at $t=0$. If the recovery processes obey second-order kinetics the plot of $(\rho - \rho_\infty)^{-1} - (\rho_0 - \rho_\infty)^{-1}$ versus t will yield a straight line. Since the values of ρ_∞ could not be determined from the data, an effort was made to obtain a straight line by choosing a reasonable value for ρ_∞ . This could be achieved for all isothermal curves of Cu, Ag, and Au in stage III [Figs. 5(a), 5(b), 5(c)]. A similar attempt to learn whether the same data could be represented by a first-order process gave negative results. Regardless of the ρ_∞ that were used, the data could not be represented by a first-order reaction.

VI. DETERMINATION OF THE ACTIVATION ENERGY SPECTRUM

It is generally accepted that, in analogy with the kinetic processes in gases and in solution, the rate of annealing follows a rate equation of the form

$$-(dn/dt) = f(n)e^{-\epsilon/kT}, \quad (3)$$

where n represents the defect concentration, t the time, T the temperature, k the Boltzmann constant, and ϵ the activation energy. If a macroscopic physical property is measured, which is proportional to the number of defects, and if only one single annealing process having a unique activation energy ϵ takes place in a given temperature region, the quantity ϵ can be determined without knowing the function $f(n)$. But these calculations can at best only give an approximate value of ϵ , if several annealing processes occur simultaneously at the same temperature.

Primak¹⁶ discusses in detail the annealing of such kinetic processes distributed in activation energy. His analysis has been applied by Magnuson, Palmer, and Koehler,¹⁷ by Bredt¹⁸ and recently by Herschbach,¹¹ and by Bauer and DeFord¹⁹ to calculate activation energy spectra for first-order processes.

Since it has been shown that the recovery in stage

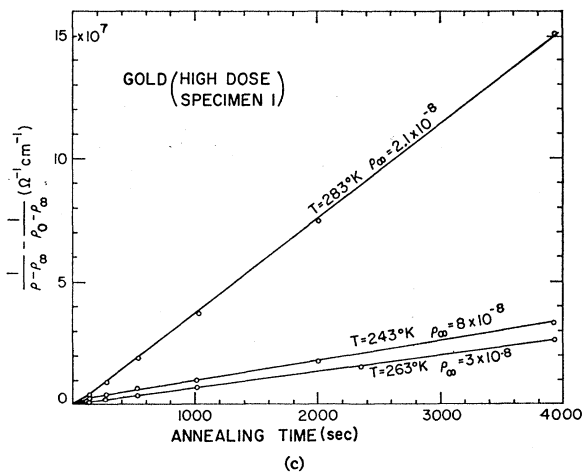
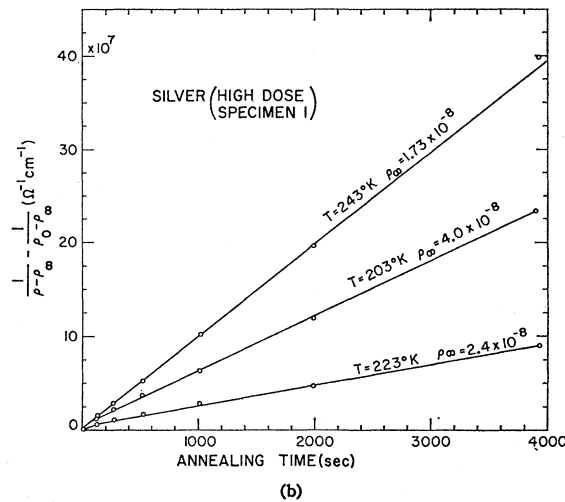
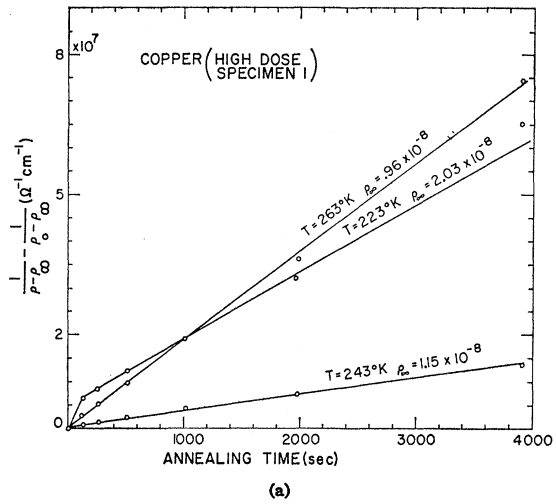


FIG. 5. $(\rho - \rho_\infty)^{-1} - (\rho_0 - \rho_\infty)^{-1}$ versus time of (a) high dose Cu annealed at 223, 243, and 263°K; (b) high dose Ag annealed at 203, 223, and 243°K; and (c) high dose Au annealed at 243, 263, and 283°K.

¹⁶ W. Primak, Phys. Rev. 100, 1677 (1955); J. Appl. Phys. 31, 1524 (1960).

¹⁷ G. D. Magnuson, W. Palmer, and J. S. Koehler, Phys. Rev. 109, 1990 (1958).

¹⁸ J. H. Bredt, doctoral thesis, Urbana, Illinois, 1960 (unpublished).

¹⁹ W. Bauer, J. DeFord, J. S. Koehler, and J. W. Kauffman, Phys. Rev. 128, 1497 (1962).

III nearly obeys a second-order rate equation, an attempt was made to determine the activation energy spectrum for a distribution of second-order processes. The calculations are based on the following assumptions:

- (a) Independent processes are distributed in activation energy.
- (b) The processes obey a second-order rate equation.
- (c) The frequency factor is constant.
- (d) The frequency factor is approximately known.

In this case Eq. (3) can be written as

$$- [dn(\epsilon)/dt] = An^2(\epsilon)e^{-(\epsilon/kT)}, \quad (4)$$

where $n(\epsilon)$ is the fractional concentration of defects annealing with activation energy ϵ and A is the frequency factor. If we assume that each defect introduces the same resistivity, then the initial resistivity introduced by defects is

$$R_0 = \int_0^\infty n(\epsilon) f d\epsilon, \quad (5)$$

where f represents the resistivity produced by 100% defects. We also assume that f does not depend on ϵ .

For the following calculations we will replace $n(\epsilon)$ by the distribution function $p(\epsilon)$, which is defined by

$$p(\epsilon) = n(\epsilon) f \quad (6)$$

and has the dimension $\Omega\text{-cm}/\text{eV}$.

Substituting $p(\epsilon)$ into Eq. (4) we get

$$-(dp/dt) = (A/f)p^2 e^{-(\epsilon/kT)}, \quad (4a)$$

and substituting into Eq. (5) we get

$$R_0 = \int_0^\infty p(\epsilon) d\epsilon. \quad (5a)$$

The solution of Eq. (4a) is

$$[p(\epsilon)]^{-1} = [p_0(\epsilon)]^{-1} + (A/f)e^{-(\epsilon/kT)t}, \quad (7)$$

where $p_0(\epsilon)$ is the value of $p(\epsilon)$ at $t=0$.

The function $p_0(\epsilon)$ can be determined by the following method: Annealing is carried out isothermally, i.e., one anneals for a time t_1 at temperature T_1 , then for a time t_2 at temperature T_2 , etc. If the distribution function was $p_0(\epsilon)$ before any annealing took place, the distribution after the first anneal is $p_1(\epsilon)$ where

$$[p_1(\epsilon)]^{-1} = [p_0(\epsilon)]^{-1} + (A/f)t_1 e^{-(\epsilon/kT_1)}. \quad (7a)$$

After the second anneal the distribution spectrum has changed to $p_2(\epsilon)$ where

$$\begin{aligned} [p_2(\epsilon)]^{-1} &= [p_1(\epsilon)]^{-1} + (A/f)t_2 e^{-(\epsilon/kT_2)} \\ &= [p_0(\epsilon)]^{-1} + (A/f)[t_1 e^{-(\epsilon/kT_1)} \\ &\quad + t_2 e^{-(\epsilon/kT_2)}]. \end{aligned} \quad (7b)$$

The spectrum after n anneals is

$$[p_n(\epsilon)]^{-1} = [p_0(\epsilon)]^{-1} + (A/f) \sum_{i=1}^n t_i e^{-(\epsilon/kT_i)}. \quad (8)$$

The defect resistivity left after n anneals is

$$R_n = \int_0^\infty p_n(\epsilon) d\epsilon, \quad (9)$$

and thus

$$R_n = \int_0^\infty \frac{p_0(\epsilon)}{1 + (A/f)p_0(\epsilon) \sum_{i=1}^n e^{-(\epsilon/kT_i)t_i}} d\epsilon. \quad (9a)$$

Our problem then is as follows: We measure the R_n at known temperatures and times. We wish to obtain the initial defect density spectrum $n_0(\epsilon) \times f$ and the frequency factor A/f .

During the n th anneal the observed change in resistivity between times t_n' and t_n'' is

$$\begin{aligned} R_n(t_n') - R_n(t_n'') &= \int_0^\infty p_0(\epsilon) \{ [1 + (A/f)p_0(\epsilon) (\sum_{i=1}^{n-1} t_i e^{-(\epsilon/kT_i)} \\ &\quad + t_n' e^{-(\epsilon/kT_n)})]^{-1} \\ &\quad - [1 + (A/f)p_0(\epsilon) (\sum_{i=1}^{n-1} t_i e^{-(\epsilon/kT_i)} \\ &\quad + t_n'' e^{-(\epsilon/kT_n)})]^{-1} \} d\epsilon. \end{aligned} \quad (10)$$

Since the integrand is appreciably bigger than zero only over a small interval of ϵ it is permissible at least for a first approximation to replace $p_0(\epsilon)$ by a constant average value $p_{01}(\bar{\epsilon})$ for this interval.¹⁸

$$\begin{aligned} R_n(t_n') - R_n(t_n'') &= p_{01}(\bar{\epsilon}) \int_0^\infty \{ [1 + (A/f)p_{01}(\bar{\epsilon}) (\sum_{i=1}^{n-1} t_i e^{-(\epsilon/kT_i)} \\ &\quad + t_n' e^{-(\epsilon/kT_n)})]^{-1} \\ &\quad - [1 + (A/f)p_{01}(\bar{\epsilon}) (\sum_{i=1}^{n-1} t_i e^{-(\epsilon/kT_i)} \\ &\quad + t_n'' e^{-(\epsilon/kT_n)})]^{-1} \} d\epsilon \\ &= p_{01}(\bar{\epsilon}) \int_0^\infty I_n' d\epsilon \end{aligned} \quad (11)$$

and

$$p_{01}(\bar{\epsilon}) = \frac{R_n(t_n') - R_n(t_n'')}{\int_0^\infty I_n' d\epsilon}$$

$\bar{\epsilon}$, the average activation energy at which annealing

occurs, is defined by¹⁸

$$\bar{\epsilon} = \frac{\int_0^{\infty} \epsilon I_n' d\epsilon}{\int_0^{\infty} I_n' d\epsilon}. \quad (12)$$

Equation (11) has been solved for $p_{01}(\bar{\epsilon})$ by the method of iteration. Successive values of $p_{01}^k(\bar{\epsilon})$ were calculated until

$$0.99 < p_{01}^k / p_{01}^{k+1} < 1.01. \quad (13)$$

The calculated activation energy spectrum consists of several segments, one for each annealing temperature. The value of the constant A/f can be determined to better than an order of magnitude, as Primak¹⁶ pointed out, by carrying out several calculations with different values of A/f until the segments fit together smoothly. The remaining uncertainty of the value of A/f produces a small error as to the exact location of p_0 in respect to the activation energy.

The first approximation to the activation energy spectrum, calculated as described above, was plotted and the curve was approximated by a number of segments of straight lines. For a second approximation it is assumed that $p_0(\epsilon)$ is a linear function of ϵ .

$$p_0(\epsilon) = p_{02} + a\epsilon. \quad (14)$$

The constant a is determined as the slope of the activation energy spectrum. Equation (11) can now be written as

$$\begin{aligned} R_n(t_n') - R_n(t_n'') &= \int_0^{\infty} (p_{02} + a\epsilon) I_n' d\epsilon \\ &= p_{02} \int_0^{\infty} I_n' d\epsilon + a \int_0^{\infty} \epsilon I_n' d\epsilon \end{aligned}$$

and

$$p_{02} = \left[R_n(t_n') - R_n(t_n'') - a \int_0^{\infty} \epsilon I_n' d\epsilon \right] / \int_0^{\infty} I_n' d\epsilon. \quad (15)$$

Equation (15) has been solved by an iteration process.

The integrals were evaluated using Gauss' formula for numerical integration. The numerical calculations were done on an IBM 7090.

VII. ACTIVATION ENERGY SPECTRA

The activation energy spectrum of the two copper specimens that received a dose of 1×10^{17} p/cm^2 is given in Fig. 6(a). It shows a complex structure of four small peaks at 0.41 eV, 0.50 eV, 0.535 eV, and 0.595 eV superposed on a continually rising background leading to a large broad peak at 0.71 eV. The activation energy spectrum of the copper specimens that were irradiated with a flux of 3.3×10^{16} p/cm^2 , shown in Fig. 6(b), shows an almost identical structure, except that the

background seems to be lower. Three small peaks occur at 0.40 eV, 0.52 eV, and 0.57 eV and another one seems to be hidden by the slope of the second peak at 0.48 eV. The large peak appears at 0.70 eV. In both cases the large peak covers 53% of the area of the total activation energy spectrum.

The activation energy spectrum for silver irradiated with a dose of 1×10^{17} p/cm^2 is given in Fig. 6(c). It has one peak at 0.43 eV and another at 0.55 eV, followed by a large broad peak at 0.67 eV, which covers 55% of the area of the total activation energy spectrum.

The activation energy spectrum of gold (irradiated with 1×10^{17} p/cm^2) seems to be much simpler than in the case of copper and silver [Fig. 6(d)]. There is one small peak near 0.49 eV and a very large broad peak with a maximum at 0.80 eV and an area of 75% of the total activation energy spectrum.

It was found that the segments of the activation energy spectra, which have been discussed above, joined best with the constant A/f equal to 1×10^{18} .

The influence of the order of reaction on the shape of the activation energy spectrum was examined by calculating $p(\epsilon)$ for these data on the assumption that the recovery follows a first-order reaction. The resulting curves differ only quantitatively from the second-order activation energy spectra. They are displaced by 0.08 eV to higher activation energies, but their structure is essentially the same.

The data, published by Overhauser¹ in his Fig. 3, have been used to calculate an activation energy spectrum shown in Fig. 6(e). It has been assumed that the recovery obeys second-order kinetics and that $A/f = 1 \times 10^{18}$. There is very good agreement between the activation energy spectra for copper obtained by two different experiments.

VIII. PULSING

Short temperature pulses were given to the gold and silver specimens, after irradiation to a dose of 3.3×10^{16} p/cm^2 . The pulse temperature and the pulse time were chosen to break up the defect moving in stage III if it has a binding energy of 0.10 eV. Negative results were obtained for both metals. The annealing proceeds just at a faster rate corresponding to the higher temperature and to the fact that there was no previous annealing.

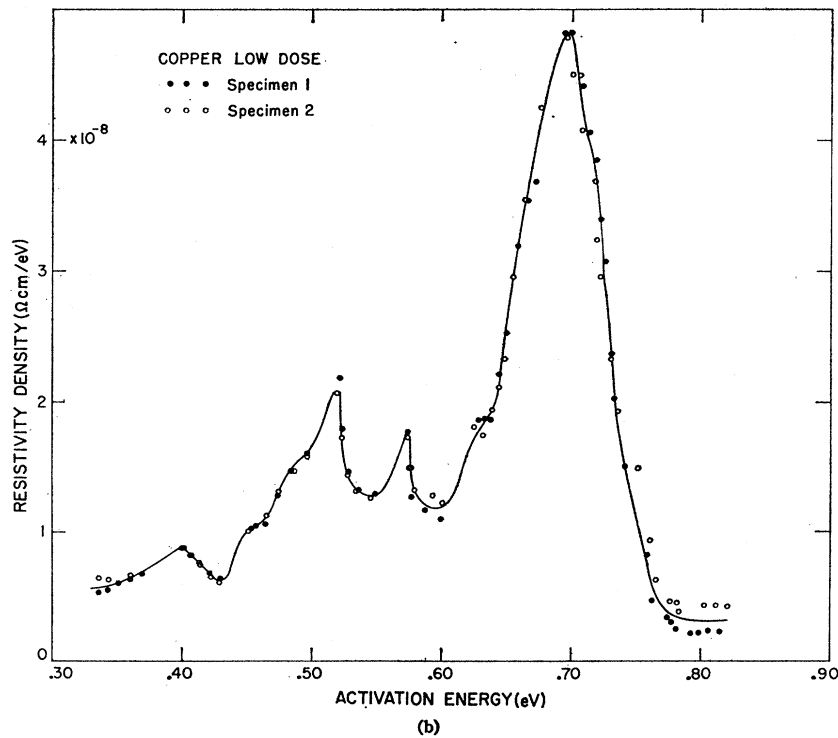
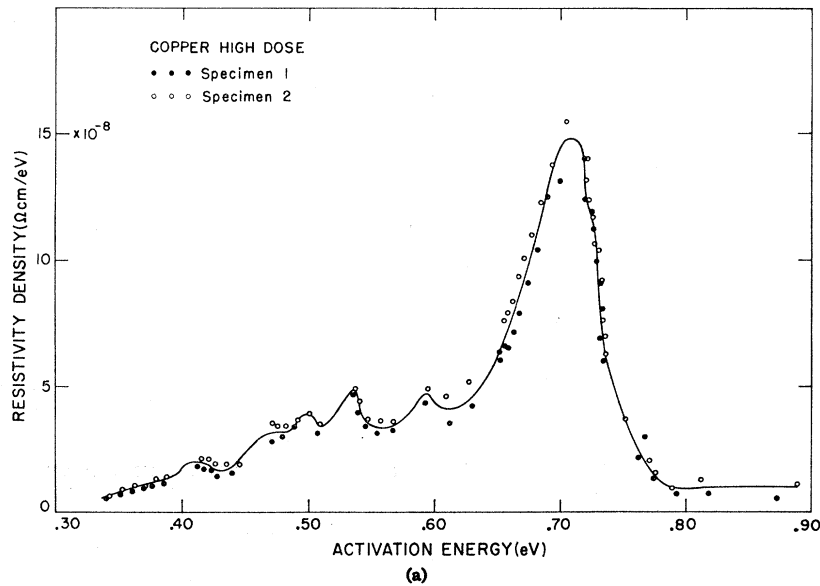
IX. DISCUSSION

Although the present experiments do not enable one to draw final conclusions concerning the nature of the annealing processes responsible for stage III in noble metals, there are certain interesting results which should be mentioned.

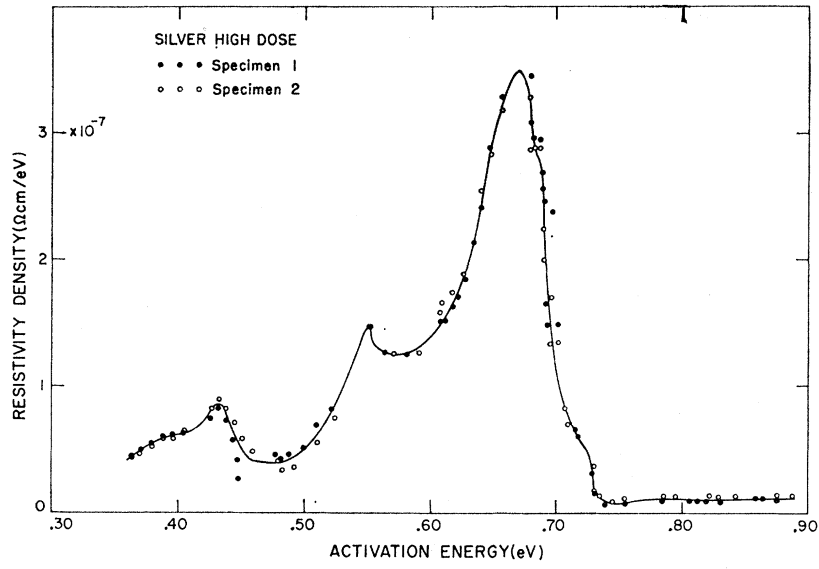
First, on the basis of the observed activation energy spectra some of the previously proposed recovery models can be excluded. In the case of silver, a comparison of the present annealing spectrum with that observed by Doyama and Koehler⁷ in quenched silver

shows clearly that in silver stage III does not occur by either vacancy or divacancy migration ($E_m^v=0.83 \pm 0.05$ eV and $E_m^{D_2}=0.57 \pm 0.03$ eV). In the case of copper the equilibrium measurements of lattice parameter and length by Simmons and Balluffi²⁰ show that stage III in copper is not associated with the migration

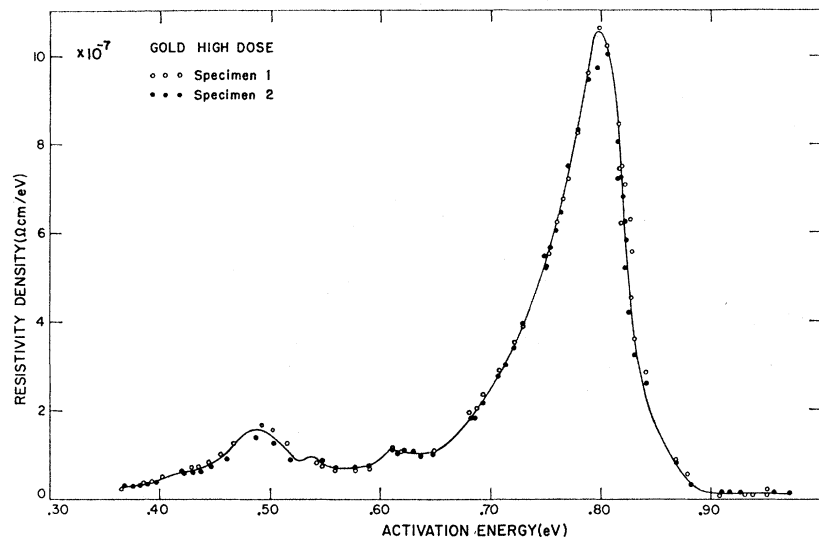
of vacancies ($E_m^v=0.88 \pm 0.04$ eV). On the other hand, the activation energy observed for stage III recovery of gold, i.e., 0.80 ± 0.04 eV, could very well be associated with the motion of single vacancies. The energy of migration of lattice vacancies in gold is observed to be 0.82 ± 0.05 eV.



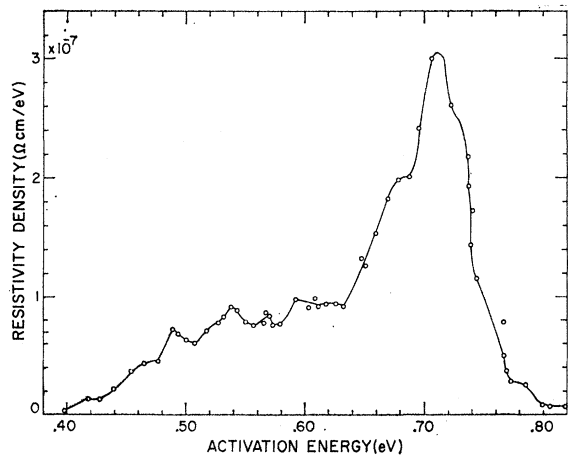
²⁰ R. O. Simmons, and R. W. Balluffi, Phys. Rev. **129**, 1533 (1963).



(c)



(d)



(e)

FIG. 6. Activation energy spectra for (a) high dose Cu; (b) low dose Cu; (c) high dose Ag; (d) high dose Au; and (e) Cu from Overhauser's data.

Second, the annealing of gold in stage III seems to differ from that observed in copper and silver. The results, which have been discussed above, already point out this difference. A comparison of the activation energy spectra of the three noble metals further supports this observation. In gold there is one rather large peak which is associated with 75% of the entire amount of resistivity that anneals.

Third, in copper and silver the annealing spectrum is decidedly more complicated than in gold. Moreover, the spectra of copper and silver seem to be at least qualitatively similar with that of silver displaced to slightly lower activation energies. Therefore, in the case of copper and silver the damage appears to recover in a number of processes with different activation energies giving rise to the observed structure of the activation energy spectra.

Meechan and Brinkman² who did electron irradiation on copper also observed more than one annealing process below 300°K. They saw one large peak centered at 298°K associated with an activation energy of 0.60 eV. In addition they observed appreciable annealing in the region from 200 to 270°K. Unfortunately, no careful examination of this low-temperature annealing was done. More recently Martin²¹ measured the stage II and III recovery of the electrical resistivity of electron irradiated high purity copper. He found three distinct peaks at 120, 190, and 270°K, and possibly a fourth peak near 230°K. No activation energies have been reported.

Fourth, the number of jumps required to annihilate the defect is smaller than one would expect if the defects were distributed uniformly. The number of jumps required to anneal out half the damage is

$$n_j = t_{1/2} \nu_0 e^{-(E_m/kT)} e^{(S/k)}, \quad (16)$$

where the annealing occurs at temperature T , $t_{1/2}$ is the time required, and S is the entropy of migration. For the following calculations it has been assumed that $e^{S/k} = 1$ and that $\nu_0 = 7 \times 10^{13}$. In gold $E_m = 0.80$ eV, $T = 260^\circ\text{K}$, and $t_{1/2} = 35$ min, so that $n_j = 66$. The total resistivity drop in the big peak is 9.3×10^{-8} $\Omega\text{-cm}$ which corresponds to a defect concentration of about 4.6×10^{-4} . Thus, in a random walk, one would expect a defect would make about 2.2×10^3 jumps. In copper and silver the number of jumps required is also smaller than one would expect if the defects were engaged in a random walk and were spread uniformly. In copper $E_m = 0.70$ eV, $T = 240^\circ\text{K}$ and $t_{1/2} = 32$ min, so that $n_j = 400$. The number of jumps required if the defects were spread uniformly would be 1.7×10^4 . In the case of silver $E_m = 0.67$ eV, $T = 220^\circ\text{K}$ and $t_{1/2} = 36$ min and one finds $n_j = 100$ and for a random walk $n_j = 7.7 \times 10^3$. Although these calculations can only be regarded as approximate, they clearly show the discrepancy between the measured and the predicted number of jumps.

²¹ D. G. Martin, Phil. Mag. 6, 839 (1961).

There seem to be two ways to understand this discrepancy: First, the defects introduced by cyclotron irradiation are produced in small clusters, but they do not interact with each other. Hence, if a defect combines with another defect in the small cluster, it does not have far to go. Let us examine the kinetics for the case that defect A (an interstitial or a diinterstitial) migrates and is annihilated when it meets defect B (a vacancy). Inside each cluster associated with a primary displaced atom we have

$$c_A = c_B,$$

where c_A is the concentration of defect A and c_B that of defect B inside the cluster. The average concentrations \bar{c}_A and \bar{c}_B are

$$\bar{c}_A = c_A(v/V) \quad \text{and} \quad \bar{c}_B = c_B(v/V) \quad \text{and} \quad \bar{c}_A = \bar{c}_B. \quad (17)$$

Here v is the volume occupied by the damage cluster and V includes v and a portion of the undamaged region between clusters.

Then

$$-(d\bar{c}_A/dt) = \bar{c}_A c_B \nu_0 e^{-(E_m/kT)} P(t) + \bar{c}_A \bar{c}_B \nu_0 e^{-(E_m/kT)} [1 - P(t)], \quad (18)$$

where $P(t)$ is the average probability that defect A recombines with a defect B of the same cluster. $P(0) = 1$ and $P(t \rightarrow \infty) \rightarrow 0$. Note that $P(t)$ is a function of the size of the cluster. The reason that one must include $P(t)$ is that even in the case of a random walk there is some probability that a defect A can escape from a cluster without recombining. Note that Eq. (18) neglects the formation of large clusters of the mobile defect. By using Eq. (17), Eq. (18) can be written as

$$-(d\bar{c}_A/dt) = \bar{c}_A c_A \nu_0 (V/v) e^{-E_m/kT} P(t) + \bar{c}_A \bar{c}_A \nu_0 e^{-(E_m/kT)} [1 - P(t)] = \bar{c}_A^2 \nu_0 e^{-(E_m/kT)} [P(t)(V/v - 1) + 1]. \quad (19)$$

Therefore the annealing occurs by a second-order process only as long as $P(t) \simeq 1$.

In small clusters, which contain 10 displaced atoms on the average, approximately 50% will be close to the surface of the cluster. In this case $P(t)$ will already change appreciably during the first few jumps and no second-order process should be observed if interaction is neglected.

A further conclusion that can be drawn from Eq. (19) is that V/v is a function of the irradiation dose assuming that the size of one cluster v does not depend on the flux (energy is constant). This implies that the apparent frequency factor A/f used for the calculation of the activation energy spectra would increase with a lower dose. This increase of A/f was not observed for the low dose copper [Fig. 6(b)]. Since these two conclusions do not agree with the reported data, the annealing inside a cluster seems to play a minor role in the recovery behavior. This is further supported

by the fact that the clusters are quite close together. For a concentration of defects of 2×10^{-4} and 20 defects per cluster, the concentration of clusters is 1×10^{-5} , and the average distance between two clusters is 100 Å or approximately 30 atomic distances. Second, if the defects are uniformly spread, but if recombination occurs with a large capture cross section, the defect migration will be random but less than $1/c$ jumps will be required for annihilation. In this case the annealing is described by the following differential equation

$$-(d\bar{c}_A/dt) = \bar{c}_A^2 \nu_0 \sigma e^{-(E_m/kT)}, \quad (20)$$

where σ is the capture cross section and is of the order of 50. We believe that this is the explanation for the low number of jumps.

It is conceivable that stage III in copper and silver involves diinterstitial migration as suggested by Corbett, Smith, and Walker²² and recently by Huntington.²³ According to theoretical calculations by Johnson and Brown²⁴ the energy of migration of such a defect is 0.26 eV and its binding energy relative to two single interstitials is 0.6 eV. It is very likely that these values are too small because the same model predicts only about 50% smaller values of the energy of motion of an interstitial and of a vacancy. Vineyard²⁵ has shown that in copper three simple configurations of close pairs of split interstitials are stable. Assuming that the di-

interstitial migrates in stage III in copper and silver, what would we expect?

Since there can be several kinds of bound di-interstitials, irrespective of whether the single interstitial is cube centered or the split (100) type, it is clear that one can have several annealing peaks.

Another possible interpretation of stage III recovery of copper and silver has been proposed by Seeger,²⁶ by Meechan, Sosin, and Brinkman³ and by Sosin and Rachal.²⁶ They have suggested that metastable crowdions move in copper at 55°K and that the stable split (100) interstitials migrate in stage III in copper, silver, and gold. They suggest that no crowdion annealing is observed in gold since the crowdion is so unstable that it immediately transforms to the stable split interstitial during the irradiation of gold.

On the basis of the present observations a complete assignment for the physical processes responsible for stage III cannot be made for all three noble metals. Further experiments will be necessary to clarify this situation.

ACKNOWLEDGMENTS

The authors would like to thank the staff of the University of Illinois cyclotron for the help in the irradiation. They also wish to thank K. S. Chen and F. Y. Cho for their assistance in this work. The computer program was written by S. W. Singer.

²² J. W. Corbett, R. B. Smith, and R. M. Walker, Phys. Rev. **114**, 1452 and 1460 (1959).

²³ H. B. Huntington, Am. J. Phys. (to be published).

²⁴ R. A. Johnson and E. Brown, Phys. Rev. **127**, 446 (1962).

²⁵ G. H. Vineyard, J. Phys. Soc. Japan **18**, Suppl. III, 144 (1963).

²⁶ A. Seeger, in *The Nature of Radiation Damage in Metals, IAEA Symposium on Radiation Damage in Solids and Reactor Materials, Venice, 1962* (International Atomic Energy Agency, Vienna, 1962).

²⁷ A. Sosin and L. H. Rachal, Phys. Rev. **130**, 2238 (1963).